Nonlinear Observer for INS Aided by Time-Delayed GNSS Measurements: Implementation and UAV Experiments

Jakob Mahler Hansen[1], Thor I. Fossen[1], Tor Arne Johansen[1]

Abstract— **A nonlinear observer structure for estimating position, velocity and attitude in a GNSS/INS system with delayed GNSS-measurements is proposed. The structure consists of an inertial measurement data buffer, a nonlinear state observer and a fast simulator. The inertial and magnetometer measurements are synchronized and delayed to coincide in time with the GNSS-measurements. The state observer will hence estimate the delayed states, and a fast simulator is employed to recover the current states using inertial measurements. The nonlinear observer is semi-global exponentially stable. The magnitude and effect of the GNSS delay is investigated, and implementation aspect of the nonlinear observer and the fast simulator are discussed. The proposed observer structure is verified by comparison to an observer without time-synchronization through use of simulations and experimental data from a UAV flight test.**

I. Introduction

Navigation of a vehicle requires knowledge about the vehicle position, velocity, and attitude, where attitude is the orientation of the vehicle in relation to a reference coordinate frame. Navigation using integration of inertial measurements and position measurements have been subjected to extensive research. Traditionally the integration between inertial navigation systems (INS) and Global Navigation Satellite Systems (GNSS) have been achieved using Kalman filters (KF) or Extended Kalman Filters (EKF). However, in recent years nonlinear observers have been introduced in the field of navigation, e.g. [1] and [2]. The nonlinear observers have the advantage of proven stability and lighter computational load.

The usual sensor requirement for nonlinear observers integrating GNSS/INS are inertial measurements of acceleration and angular velocity by an IMU, and position measurements by a GNSS-receiver. Often also magnetometer measurements and GNSS velocity measurements are desired if not required, [3]. The GNSS-measurements suffers from a delay due to the computational load of estimating the position by the receiver, as well as serial data communication between receiver and computer. This delay is often neglected but can have a magnitude of up to several hundred milliseconds. A delay of this magnitude can rightfully be ignored at low speed applications like ships or pedestrian applications, while at high speed applications such as automated landing of Unmanned Areal Vehicles (UAVs) the position used in the integration might be several meters off.

For GNSS/INS integration the delay will affect the position measurements, potentially leading to the use of outdated measurements and delayed estimates. Large delays in feedback control loops result in performance limitations, and hence it is of interest to reduce the impact of a delay in GNSS/INS integration.

In terms of time delay estimation, multiple approaches have been covered by [4] using discrete-time analysis. An experimental setup for latency determination and compensation is described by [5]. Within the field of delayed systems [6] investigates stability and observer design, while [7] takes the observer approach of an extended Kalman filter to gain asymptotic stability. The effect of a large time synchronization error in a loosely coupled GPS-aided INS is studied by [8], where the time synchronization error is included as a state in a Kalman filter. [9] investigates the effects of time synchronization errors in GNSS/IMU systems. Within linear SISO-models [10] shows stability of time-delayed systems. An algorithmic methodology to ensure stability is presented in [11]. Similar methods and architectures for time-delay

[1]Department of Engineering Cybernetics, Norwegian University of Science and Technology, 7491 Trondheim, Norway. jakob.mahler.hansen@itk.ntnu.no, thor.fossen@ntnu.no, tor.arne.johansen@itk.ntnu.no

compensation are discussed in [12] on integrated navigation. Latency and computational delay of GPS systems is investigated in [13] where the GPS delay was found to be several hundred milliseconds, furthermore a modified Extended Kalman filter approach was proposed for attitude estimation. Recently a study on the effects of time-delays in feedback loops on a quadrotor helicopter has been carried out by [14]. Also recent work by [15]–[17] propose an observer-predictor approach for delayed GNSS and magnetometer measurements consisting of an observer for delayed position and a predictor estimating the current position based on the delayed estimate.

In the present paper we study an online estimation of the current position and velocity from delayed GNSS-measurements and current inertial measurements. The work is based on a nonlinear observer proposed in [3], [18] and [19], with proven stability results, attitude estimation using quaternions and gyro bias estimation. We propose an approach where the inertial and magnetometer measurements are delayed at the input of the observer with a delay corresponding to the GNSS-delay, resulting in delayed position and linear velocity estimates. The current position and velocity estimates are computed by integrating IMU data starting at the delayed estimates through a fast simulator.

Initially the time-delay of a typical GNSS receiver is described in Section II, followed by a system description in Section III, and the observer structure in Section IV. The complete observer structure is simulated in Section V, while experimental results are shown in Section VI, with Section VII concluding the paper.

II. GNSS Time delay

In the following the GNSS receiver delay will be considered, covering the delay arising from the signal enters the receiver until it is available to the user. The receiver delay consists of multiple parts: conversion, estimation and transmission, where the signal is first converted from the wave-signal to the receiver format, then the positions are estimated and finally the data is transmitted to the user. In order to estimate the delay two signals are used: a pulse-per-second (PPS) and the data transmission. The PPS signal is offered by most GNSS-receivers and consists of a signal giving a pulse at $1\ Hz$ synchronized with GNSS-time, such that the pulse has a rising edge every time the GNSS-time increments with a second. It is assumed that the PPS signal is not delayed on the receiver. The data transmission includes the raw measurements, time stamps, position estimates, etc.

In the ideal case the computed position output would be available to the user at the same time as the PPS signal. The rising edge of the PPS signal signifies the time of validity (TOV) of the measurement. However the computed position output is available at a later time denoted time of arrival (TOA) when the entire computed position output has been transmitted by the receiver. The receiver delay can be observed as the time between the rising edge of the PPS signal and the last falling edge of the data, in other words the time between TOV and TOA, see Fig. 1.

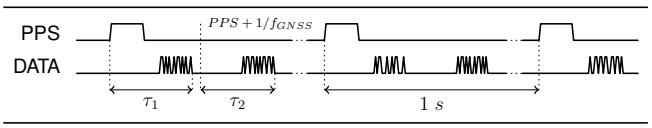

Fig. 1: Visualization of PPS and data signal on a time-scale, depicting the time-delay estimation for a GNSS-receiver.

The described approach covers the situation when the data signal has a frequency of $1\ Hz$, i.e. the same as the PPS signal. If the data signal has a higher frequency than the PPS signal, there are multiple data-packages within one PPS-period. In this case the first delay is determined as described above, while the subsequent delays are estimated as the time between the PPS time shifted with the GNSS frequency (i.e. $PPS + n/f_{GNSS}$ for $n = 0, 1, \ldots, f_{GNSS} - 1$) and the last falling edge of each data-package.
If the data frequency is lower than that of the PPS signal, or a lot higher then accurate determination of the time-delays will require knowledge of the approximate delay, as it will be difficult to relate the data-package to the appropriate PPS rising edge.

A. Case Study: u-Blox LEA-6T

To illustrate the time-delay estimation procedure a case study on the u-Blox LEA-6T receiver will be conducted. The receiver used is in an evaluation kit, EVK-6T, which has PPS and data signal readily available on a RS232 transmission. A custom printed circuit board is designed with a PIC32 microcontroller, ensuring accurate time stamping by use of input capture on a 16 bit timer. The rising edge of the PPS signal and last falling edge of the data signal is time stamped by the microcontroller as the TOV and TOA, respectively. The time-delay is then computed as the time between the two time stamps, and the IMU data are also time-stamped and synchronized with the PPS.

The content of the data output can be selected from multiple options in the u-Blox receiver. A test is carried out where the RAW package of the u-Blox, containing pseudo ranges and carrier phase frequency measurements, is used as the data signal to estimate the time-delay experienced in tight GNSS/INS integration. The test is carried out over one hour with measurements of 1 Hz, and the results are depicted in Fig. 2.

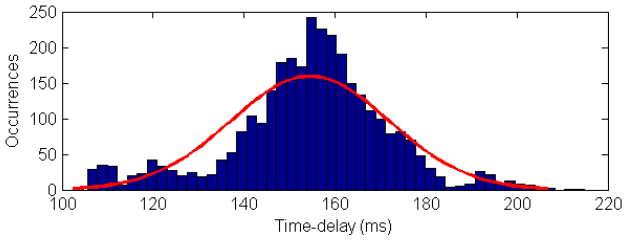

Fig. 2: Time-delay measurements over one hour with 1 Hz measurements, using u-Blox EVK-6T.

Fig. 2 shows the observed time-delays and their occurrences, along with a superimposed Gaussian distribution. The average value of the distribution is 154.5 ms with standard deviation 17.4 ms.

The observed time delay will vary with receiver type and parameters of internal filters, as well as the satellite constellation (specifically the number of satellites).

III. Problem Formulation

The focus of this paper is to estimate the position, linear velocity and attitude (PVA) of a vehicle by integrating inertial measurements in the BODY frame aided by delayed GNSS position measurements. If the integration process does not take delay on the position measurements into account the PVA estimates will degenerate, as the comparison between the measured and estimated position will depend on the time delay. We have investigated the implementation aspects of a INS/GNSS integration method for handling constant and known time delays on the GNSS measurements. The nonlinear observer is based on [19], with a change of coordinate frame from Earth-Centred-Earth-Fixed (ECEF) to (North-East-Down) NED.

The position, linear velocity, attitude and gyro bias is represented as p^n, v^n, q_b^n and b^b, respectively. The attitude is expressed in the unit quaternion representation and describes the rotation from BODY to NED frame. The position, linear velocity and attitude is collectively called the navigation vector.

The system equations describing the navigation vector and gyro bias is delayed with $\tau = \tau_{GNSS} > 0$ to match the validity of the GNSS measurements,

$$\dot{p}^n(t-\tau) = v^n(t-\tau), \tag{1}$$
$$\dot{v}^n(t-\tau) = g^n + R(q_b^n(t-\tau))f^b(t-\tau), \tag{2}$$
$$\dot{q}_b^n(t-\tau) = \frac{1}{2}q_b^n(t-\tau) \otimes \bar{\omega}_{ib}^b(t-\tau), \tag{3}$$
$$\dot{b}^n(t-\tau) = 0, \tag{4}$$

where g^n is the NED gravitational vector. The specific force and angular velocity in BODY frame are f^b and ω_{ib}^b. The operator $S(\cdot)$ and $\otimes$ are the skew-symmetric matrix and the Hamiltonian quaternion product, respectively. The operation $\bar{x} = [0; x]^T$ refers to the quaternion with vector part x and zero real part.

A. Sensor Configuration Assumptions

It is assumed that the following sensor data are available:

- Position measurement experiencing a time delay, measured by the onboard GNSS-receiver, $p^e(t-\tau)$ in the ECEF frame.
- Specific force of the vehicle, measured by the onboard IMU, f^b.
- Angular velocity of the vehicle experiencing a bias, b^b, measured by the onboard IMU, $\omega_{ib,IMU}^b = \omega_{ib}^b + b^b$.

- Magnetic field measurement of the Earths magnetic field observed from the vehicle, measured by the onboard magnetometer, m^b.

IV. Nonlinear Observer

The nonlinear observer consists of an attitude estimation part that also determines the gyro bias, and a position and linear velocity part, which apply the position error as an injection term. In the following the observer proposed in [19] will be used in a time-delayed version where the time argument is shifted from present time, t, to delayed time, $t-\tau$, to match the delay experienced by the GNSS-receiver.

The attitude estimation expressed in quaternion representation is given as, [1], [18]:

$$\begin{aligned}\dot{\hat{q}}_b^n(t-\tau) = \frac{1}{2}\hat{q}_b^n(t-\tau) \otimes \big(\bar{\omega}_{ib,IMU}^b(t-\tau) \\ - \bar{\hat{b}}^b(t-\tau) + \bar{\hat{\sigma}}(t-\tau)\big),\end{aligned} \tag{5}$$

$$\dot{\hat{b}}^b(t-\tau) = \text{Proj}\left(\hat{b}^b(t-\tau), -k_I\hat{\sigma}(t-\tau)\right), \tag{6}$$

where $k_I > 0$ is a constant tuning parameter and $\text{Proj}(\cdot)$ refers to the projection function, limiting the gyro bias estimate to a compact set limited by a sphere with radius M_b, such that $\|\hat{b}^b\| \leq M_b$. The injection term $\hat{\sigma}$ is determined from two vectors in the BODY frame (v_1^b and v_2^b) and their corresponding vectors in the NED frame (v_1^n and v_2^n):

$$\begin{aligned}\hat{\sigma}(t-\tau) := k_1 v_1^b(t-\tau) \times R_q^T v_1^n(t-\tau) \\ + k_2 v_2^b(t-\tau) \times R_q^T v_2^n(t-\tau),\end{aligned} \tag{7}$$

here $R_q = R(\hat{q}_b^n(t-\tau))$, furthermore $k_1 \geq k_p$ and $k_2 \geq k_p$ are constant gain factors for some $k_p > 0$, and $\times$ denotes the cross product of two vectors. The vectors included in $\hat{\sigma}$ can be chosen in various ways. Here they will be given as:

$$v_1^b = \frac{f^b}{\|f^b\|}, \quad v_2^b = \frac{m^b}{\|m^b\|} \times v_1^b \tag{8}$$

$$v_1^n = \frac{\hat{f}^n}{\|\hat{f}^n\|}, \quad v_2^n = \frac{m^n}{\|m^n\|} \times v_1^n. \tag{9}$$

The vectors are based on normalised measurements of the specific force and magnetometer measurements of the vehicle and the corresponding vectors in the NED frame. The specific force in NED frame is estimated with position and velocity as:

$$\begin{aligned}\dot{\hat{p}}^n(t-\tau) = \hat{v}^n(t-\tau) \\ + \theta K_{pp}(R_\Theta^T p^e(t-\tau) - \hat{p}^n(t-\tau)),\end{aligned} \tag{10}$$

$$\begin{aligned}\dot{\hat{v}}^n(t-\tau) = \hat{f}^n(t-\tau) + g^n(\hat{p}^n(t-\tau)) \\ + \theta^2 K_{vp}(R_\Theta^T p^e(t-\tau) - \hat{p}^n(t-\tau)),\end{aligned} \tag{11}$$

$$\begin{aligned}\dot{\xi}(t-\tau) = -R_q S(\hat{\sigma}(t-\tau)) f^b(t-\tau) \\ + \theta^3 K_{\xi p}(R_\Theta^T p^e(t-\tau) - \hat{p}^n(t-\tau)),\end{aligned} \tag{12}$$

$$\hat{f}^n(t-\tau) = R_q f^b(t-\tau) + \xi(t-\tau), \tag{13}$$

where $R_\Theta = R_n^e(\Theta_{en})$. The transformation of the measured position, $p^e(t-\tau)$, from ECEF to NED is achieved with the rotation matrix $R_n^e(\Theta_{en})$, where $\Theta_{en} = [l, \mu]^T \in S^2$ formed by the longitude l and latitude μ, [20].
The constant parameter $\theta \geq 1$ is a tuning factor. The gain matrices K_{pp}, K_{vp}, and $K_{\xi p}$ must be chosen to satisfy $\mathcal{A} - \mathcal{K}\mathcal{C}$ being Hurwitz where:

$$A = \begin{bmatrix} 0 & I_3 & 0 \\ 0 & 0 & I_3 \\ 0 & 0 & 0 \end{bmatrix}, \mathcal{K} = \begin{bmatrix} K_{pp} \\ K_{vp} \\ K_{\xi p} \end{bmatrix}, \mathcal{C} = \begin{bmatrix} I_3 \\ 0 \\ 0 \end{bmatrix}^T.$$

The shifting of the observer in time does not affect the properties of the observer and the stability proof follows directly from [19] resulting in semi-global exponentially stability.

A. Observer structure

The time-delayed state observer is included in an observer structure that consists of the sensor suite, data buffers, and a fast simulator. The objective of the fast simulator is to estimate the current position and velocity from the delayed estimates. The proposed observer structure is shown in Fig. 3. The data buffer is placed at the input to the attitude estimation, so as to not affect the tuning and stability of the state observer. By delaying the inertial measurements, the observer apply the integration to inertial and position measurements of the same instance.

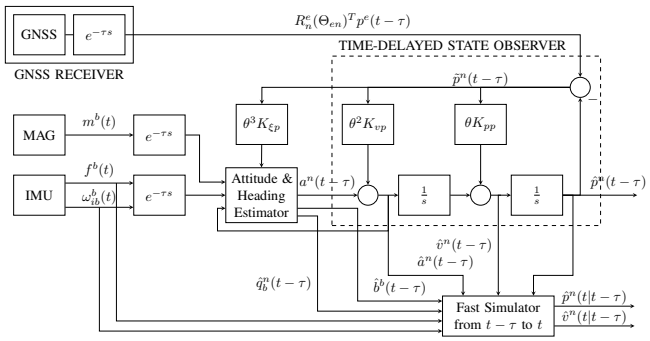

Fig. 3: Observer structure consisting of sensor suite, input delays, attitude estimator, time-delayed state observer, and fast simulator. The specific force estimate and the ξ state are included in the Attitude & Heading Estimator block for simplicity.

B. Fast simulator

The fast simulator is necessary to estimate the current measurements from the estimated delayed measurements. It is desired to iterate through time from $t-\tau$ to t at a time-scale much faster than the observer update rate. The proposed fast simulator is derived by using the transition matrix of a double integrator system, presented here in its general form:

$$\dot{x} = Ax + Bu, A = \begin{bmatrix} 0 & I \\ 0 & 0 \end{bmatrix}, B = \begin{bmatrix} 0 \\ I \end{bmatrix}, \quad (14)$$

$$x(t) = e^{A(t-t_0)}x(t_0) + \int_{t_0}^{t} e^{A(t-s)}Bu(s)ds. \quad (15)$$

In the present case let $t_0 = t-\tau$ and $u(t) = a^n(t) = R(\hat{q}_b^n(t))f^b(t) - g^n$. The current position and velocity can then be estimated as:

$$\hat{v}^n(t|t-\tau) = \hat{v}^n(t-\tau) + \int_{t-\tau}^{t} a^n(r)dr, \quad (16)$$

$$\hat{p}^n(t|t-\tau) = \hat{p}^n(t-\tau) + \tau\hat{v}^n(t-\tau) + \int_{t-\tau}^{t}\int_{t-\tau}^{s} a^n(r)drds, \quad (17)$$

where $\hat{p}^n(t-\tau)$ and $\hat{v}^n(t-\tau)$ are estimated by the state observer, and f^b is supplied by the IMU. The attitude estimates used in the fast simulator requires a duplicate of (5) where inertial data from time $t-\tau$ to t is used. Another approach is to use the fast simulator as post-processing to the attitude and translational motion observers, where the attitude estimates can be stored in a buffer. The approach of choice depends on computational power available as a trade off of post-processing.

C. Implementation considerations

When implementing the observer structure for online operation there are a couple of issues to resolve. One of these is the discretization of the nonlinear observer. Here we used the *Corrector-Predictor Representation of Nonlinear Observers* described in [20]. The Corrector-Predictor (CP) approach is beneficial when implementing systems with multiple sensors that have different sample frequencies. This is typically the case as GNSS-receivers have sample frequencies of $1-10\ Hz$ and IMUs usually have $100-1000\ Hz$. The idea behind the CP approach is to implement differential equations with linear injection terms in two steps: a corrector and predictor step, where the predictor use simulation of the state variables using the transition matrix and nonlinear elements of the equations, while the corrector step uses the injection to update the states. The predictor step is carried out at the observer frequency (usually mimicking the fastest sensor frequency) while the corrector step is only carried out when a new measurement arrives, [20]:

$$\begin{aligned} \text{Corrector:} \quad & \hat{x}(k) = \bar{x}(k) + K_d\left(y(k) - \bar{y}(k)\right) \\ \text{Predictor:} \quad & \bar{x}(k+1) = \hat{x}(k) + hf(\hat{x}(k), u(k)), \end{aligned}$$

where the corrector updates the state $\bar{x}(k)$ to $\hat{x}(k)$ when new GPS measurements are available. The predictor use the nonlinear model $\dot{x} = f(x,u)$ to predict the estimate between GPS measurements. The weighting depends on the sample frequency, h, of the sensors, where $K_d = h\mathcal{K}$.

The drawback of the CP approach is that it is limited to differential equations with linear injection terms. The authors implemented the estimate of position, (10), linear velocity, (11), and ξ, (12), using the CP approach. The remaining differential equations, (5) and (6) were implemented using Euler integration.

Implementing the time-delays for the inertial measurements online requires the option for storing the data from the time it is obtained to the time it is needed by the attitude estimator. This data buffer has the length of the time-delay. One way to do this is to have vectors of a length corresponding

to the number of measurements arriving in a time interval matching the delay. The measurements can then be added to the vector in a first-in-first-out approach, such that new measurements are added at the top and the attitude estimator apply the bottom-most measurements. If the delay is large or the inertial sensors have high rates this approach can be computationally hard as the amount of data being shifted in every iteration is of considerable size. Another approach is to save the data to storage when new inertial measurements arrive and reading from storage when data is needed for the observer. The speed and computational requirements of this approach depends on the writing and reading speed of the online system. In [15] a third approach is presented for use in the predictor where two copies of the delayed equations exist and the observer periodically switches between these to avoid unbounded variables.

Storing of the inertial measurements also implies another constraint, as it will only be possible to store the measurements a fixed number of samples, m. The time-delay of the inertial measurements and prediction in the fast simulator will therefore be an approximation of the GNSS-delay based on a fixed number of samples. The approximation will be a rounding to nearest integer $m = \tau / f_{system}$, where f_{system} is the rate of the observer discrete-time implementation. As the observer equations are often implemented at the same rate as the inertial measurements, this implies a benefit of fast IMUs for systems with small or accurate time delays. For IMUs with high sample rate this is an issue of negligible proportions.

V. Simulation

In order to verify the observer structure implementation, some test data is created and several scenarios investigated.

The input measurements required for testing include; m^b, f^b, ω_{ib}^b, and p^e, along with the timing of the measurements from the sensors. It is assumed that the inertial measurements (m^b, f^b, and ω_{ib}^b) are measured simultaneously with a frequency of $410\ Hz$. The position measurements is assumed to have a frequency of $5\ Hz$ and to form a helix with center in $(l, \mu) = (10.32, 60.20)$, where l is longitude and μ is latitude. The radius of the path is 0.004 degrees corresponding to approximately $450\ m$ in latitude and $225\ m$ in longitude. Furthermore, the height increases with a rate of $0.05\ m/s$.

The inertial measurements are constant with: $m^b = [0.015, 0.015, 0.015]^T\ T$, $f^b = [1, 0.2, -9.81]^T\ m/s^2$, and $\omega_{ib,IMU}^b = [0, 0, \pi/2]^T$ rad$/s$. The parameters used for the simulations are: $M_b = 0.0087$, $k_1 = 0.05$, $k_2 = 0.05$, $k_I = 0.004$, $\delta = 0.001$, $\theta = 1$, $K_{pp} = 1.8 I_3$, $K_{vp} = 1.2 I_3$, and $K_{\xi p} = 0.5 I_3$.

Throughout the simulations the proposed observer structure will be compared with the conventional observer. The conventional observer is here defined as [3], [19]. It will therefore be similar to the proposed observer structure except that the inertial measurements will not be delayed and the position estimate will be the output of the state observer and not the fast simulator. The same parameters will be used for the proposed observer structure and the conventional observer.

A. *Simulation with* $\tau = 0.15\ sec$

A simulation is carried out with a delay of $\tau = 0.15\ s$ and the results from the proposed observer structure is depicted in Fig. 4 where the error from the proposed observer structure is shown along side the error of the conventional observer.

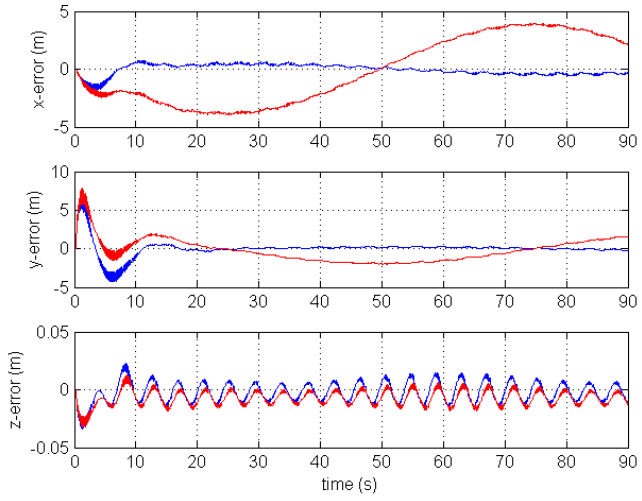

Fig. 4: Position estimate errors from a simulation with $\tau = 0.15\ s$. The error of the proposed observer structure is shown in blue and error from the conventional observer in red.

The error of the proposed observer structure is

considerably smaller than that of the conventional observer. Both error signals have initial oscillations that fades away within 20 seconds. The stationary states of the error signals have sinus-wave characteristics due to the sinusoid position reference.

The fast simulator can be verified by comparing the $\hat{p}^n(t-\tau)$ from the state delayed observer and the predicted state $\hat{p}^n(t|t-\tau)$, as done in Fig. 5. The left part of Fig. 5 shows the position estimate

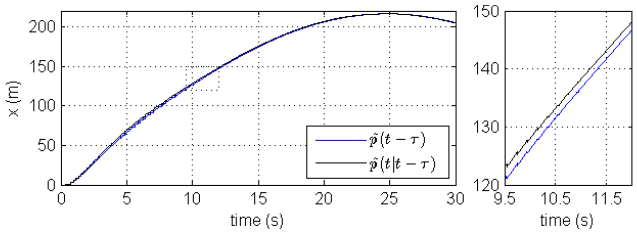

Fig. 5: Verification of the fast simulator showing the delayed position estimate at time $t-\tau$, in blue, being predicted at time t, in black.

for the x-position, where a section of the graphs have been highlighted, with a dashed box, which is shown in more detail on the right side. The predicted position precedes the delayed position estimate with an offset in time seen approximately to be the size of the GNSS-delay.

B. Simulation with uncertainty on the time-delay

In the previous simulation we considered perfect correspondence between the GNSS-delay and the user implemented input delay of inertial measurements. Let us consider the case where perfect knowledge of the GNSS-delay is not available. In the following there will be a distinction between the GNSS-delay, τ, and inertial delay, $\hat{\tau}$, where $\tau \neq \hat{\tau}$, which results in a substitution of τ to $\hat{\tau}$ in (5)–(7), (10)–(13), and (16)–(17), with the exception of the position measurements: $p^e(t-\tau)$. The results of a simulation with $\tau = 0.15\ s$ and $\hat{\tau} = 2\tau = 0.30\ s$ is shown in Fig. 6.

The errors of the conventional observer are virtually unchanged while the error of the proposed observer has increased to comparable magnitude. While the state estimates of the delayed state observer converges the fast simulator will predict the positions with $\hat{\tau}$, and the position errors of the proposed observer will therefore have a bias. The

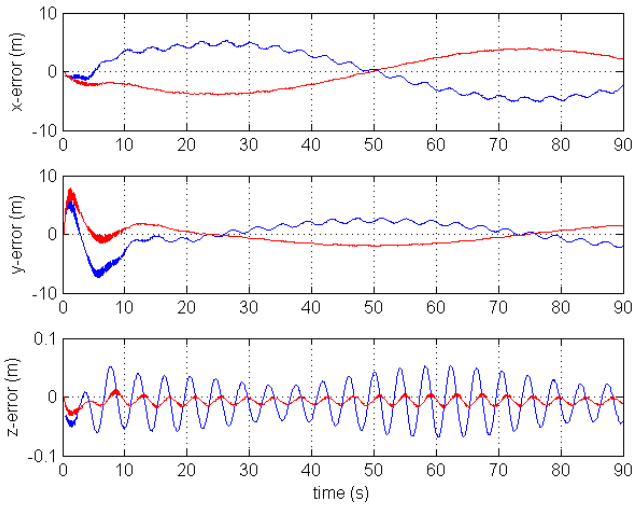

Fig. 6: Estimation errors of position with uncertainty of the time-delay. The conventional observer error is shown in red while the error of the proposed observer is blue.

fast simulator is dependent on a good estimate of the time-delay.

Comparing the conventional observer with the proposed observer structure it becomes evident that the proposed observer can handle uncertainties of the time-delay up to a factor of two before having positioning errors of the same magnitude as the conventional observer.

VI. Experimental Verification

This section presents experimental results of the proposed observer obtained using data acquired from a flight with a Penguin B UAV, see Fig. 7. The max level speed of the UAV is $36\ m/s$ which corresponds to distance between measured and actual position of $5.4\ m$ at time-delay of $0.15\ s$ as was observed in Section II. The flight was conducted at Eggemoen airport in Norway in November 2014. The part of the flight shown here is the 180 seconds around take off.

The UAV is equipped with a payload consisting of multiple sensors (GNSS-receiver, IMUs, magnetometer, altimeter), time synchronization hardware and an onboard computer for data logging, see Fig. 8. In addition to the payload sensor the autopilot logs sensor and flight data for comparison. The time synchronization hardware is a custom printed

Fig. 7: UAV Platform: Penguin B

circuit board with a microcontroller as described in Section II-A.

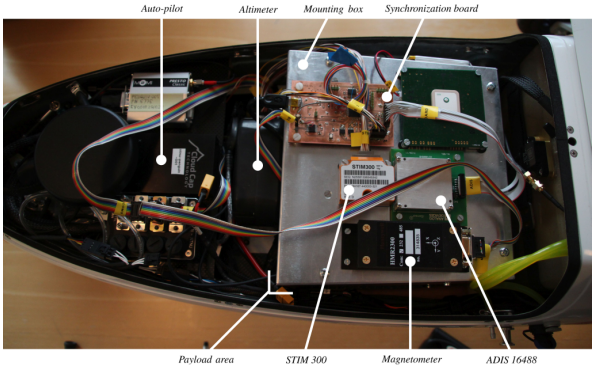

Fig. 8: Payload of the UAV consisting of multiple sensors, onboard computer and synchronization hardware. The computer and GNSS-receiver is located in the aluminium casing.

The sensors used in the following are a u-Blox EVK-6T GNSS-receiver, logging the GPS position of the UAV with a frequency of $5\ Hz$ and an ADIS 16488 IMU, logging acceleration, angular velocities and magnetometer data in three axes with a frequency of $410\ Hz$. The inertial measurements are filtered with a Butterworth low-pass filter to reduce the effect from the combustion engine vibrations. The filter is 5th order with cut-off frequency at $6\ Hz$.

The time-delay is assumed to be constant at $\tau = 0.15\ s$ throughout the flight. The parameters used for the observer are: $M_b = 0.0087$, $k_1 = 0.01$, $k_2 = 0.01$, $k_I = 0.004$, $\delta = 0.001$, $\theta = 1$, $K_{pp} = 2.0I_3$, $K_{vp} = 1.0I$, and $K_{\xi p} = 0.5I$.

The path of the UAV estimated by the GPS receiver is shown in Fig. 9 with the estimated position. The attitude estimates and estimation errors

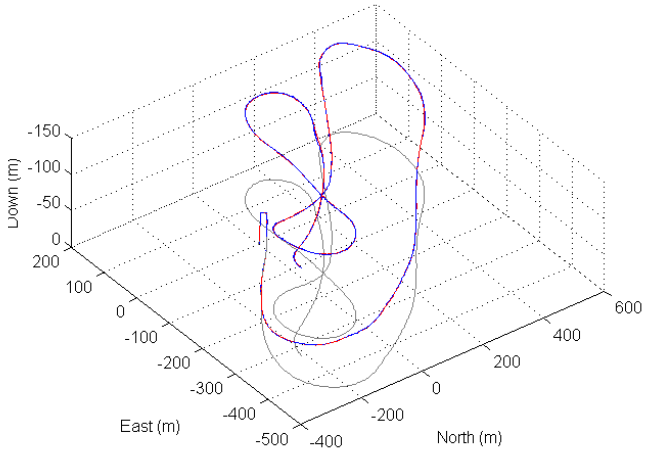

Fig. 9: 3-D path of the UAV with take off from origo. The path measured by the GNSS-receiver in red, the estimated position in blue. The grey trajectory is the ground projection of the the measured positions.

of the position by the proposed observer and the conventional observer without delay compensation are shown in Fig. 10 and Fig. 11, respectively.

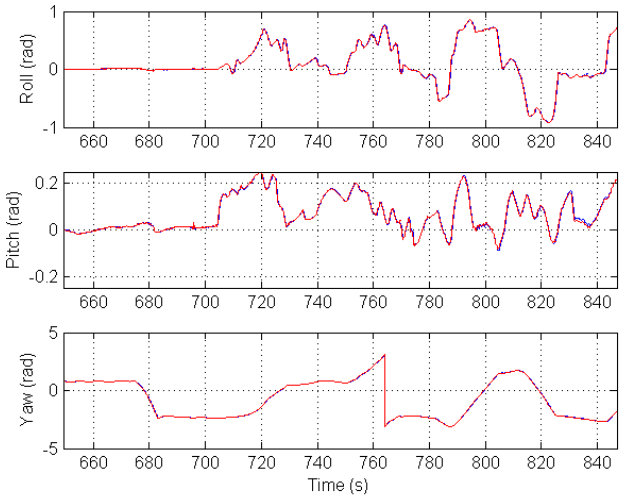

Fig. 10: The attitude estimates of the proposed observer structure (blue) and the conventional observer without delay compensation (red).

The attitude estimates are similar for the proposed and conventional observer, except that the estimates of the conventional observer are valid

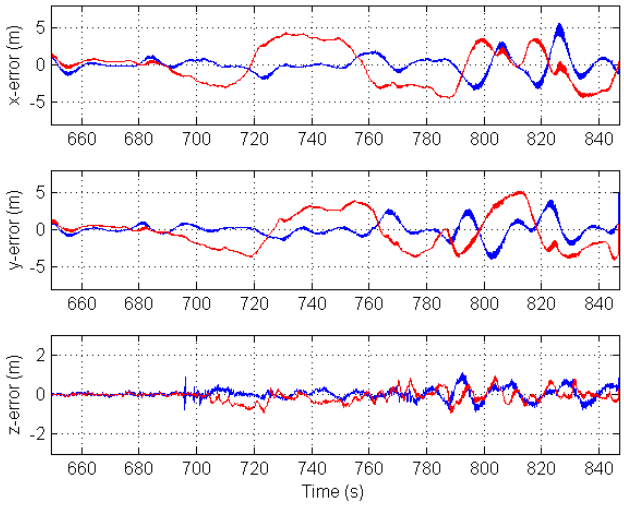

Fig. 11: The estimation errors of the proposed observer structure (blue) and the conventional observer without delay compensation (red).

before the proposed observer estimates, as expected. When computing the estimation errors, the conventional and proposed observer are compared to a reference consisting of the estimation offered by an implementation similar to the conventional observer, which does not experience a delay on the GPS measurements. Note that the only difference between the conventional observer and the reference is a delay of the GPS measurements. However, it is only possible to compute the reference in post-processing as it requires future measurements. The position estimation errors are within 5 meters during most of the flight with few deviations. The two observers give similar results for low speed (before take-off at approximately $690\ s$, whereas for higher speeds the proposed observer structure have smaller errors than the conventional observer without delay compensation. The variance of the error signals using the proposed observer structure are: $\text{Var}\left(p(t) - \hat{p}(t|t-\tau)\right) = [1.42,\ 1.14,\ 0.06]$, whereas the conventional observer without delay compensation gives $\text{Var}\left(p(t) - \hat{p}_{trad}(t-\tau)\right) = [6.10,\ 5.55,\ 0.08]$. The error of the proposed observer structure is in general smaller, with the exception of the altitude estimate where the approaches are similar.

VII. Conclusive Remarks

An observer structure consisting of an inertial measurement data buffer, a nonlinear state observer and a fast simulator was proposed, to estimate position, linear velocity and attitude in a GNSS/INS system with delayed GNSS-measurements. The inertial measurements were delayed to coincide in time with the GNSS-measurements, while the fast simulator propagates the delayed position estimate based on the delayed state observer. The magnitude and effect of the GNSS-delay have been discussed as well as implementation issues of the observer and fast simulator. The effect of the proposed observer structure have been verified through simulations, where it was compared to the conventional observer without delay compensation. It was seen that the proposed observer structure was superior in accuracy at delays of the measured magnitude. The implementation was tested on experimental data from a flight with a Penguin B UAV.

Acknowledgment

This work was supported by the Norwegian Research Council (grants no. 221666 and 223254) through the Centre of Autonomous Marine Operations and Systems (AMOS) at the Norwegian University of Science and Technology.

The authors are grateful for the assistance provided by the UAV engineers at NTNU and Maritime Robotics AS, in particular Lars Semb and Carl Erik Stephansen. Significant contributions to the construction of the UAV payload was made by the rest of the team at NTNU, in particular Sigurd Albrektsen, Kasper T. Borup and Lorenzo Fusini.

References

[1] R. Mahony, T. Hamel, and J.-M. Pflimlin, "Nonlinear Complementary Filters on the Special Orthogonal Group," *IEEE Transactions on Automatic Control*, vol. 53, No 5, pp. 1203–1218, 2008.

[2] B. Vik and T. I. Fossen, "A Nonlinear Observer for Integration of GPS and INS Attitude," *Proceedings of ION GPS'99, Nashville, TN, 14-17 September*, vol. -, pp. –, 1999.

[3] H. F. Grip, T. I. Fossen, T. A. Johansen, and A. Saberi, "A Nonlinear Observer for Integration of GNSS and IMU Measurements with Gyro Bias Estimation," *Proceedings of the American Control Conference*, vol. -, p. 6, 2012.

[4] G. Jacovitti and G. Scarano, "Discrete Time Techniques for Time Delay Estimation," *IEEE Transactions on Signal Processing*, vol. 41, pp. 525–533, 1993.

[5] P. D. Solomon, J. Wang, and C. Rizos, "Latency Determination and Compensation in Real-Time GNSS/INS Integrated Navigation Systems," *International Archives of the Photogrammetry, Remote Sensing and Spatial Information Sciences*, vol. XXXVIII-1/C22, pp. –, 2011.

[6] K. Gu and S.-I. Niculescu, "Advanced Topics in Control Systems Theory," *Chapter 4 in Lecture Notes in Control and Information Science (A. Loria, F. Lamnabhi-Lagarrigue, E. Panteley)*, vol. 328, pp. 139–170, 2006.

[7] T. Raff and F. Allgöwer, "An EKF-Based Observer For Nonlinear Time-Delay Systems," *American Control Conference*, vol. -, p. 4, 2006.

[8] I. Skog and P. Händel, "Time Synchronization Errors in Loosely Coupled GPS-Aided Inertial Navigation Systems," *IEEE Transactions on Intelligent Transportation Systems*, vol. 12, pp. 1014–1023, 2011.

[9] ——, "Effects of time synchronization errors in GNSS-aided INS," in *Position, Location and Navigation Symposium, 2008 IEEE/ION*, May 2008, pp. 82–88.

[10] P. Albertos and P. Garcia, "Predictor-observer-based control of systems with multiple input/output delays," *Journal of Process Control*, vol. 22, pp. 1350–1357, 2012.

[11] A. Papachristodoulou, M. Peet, and S. Lall, "Constructing Lyapunov-Krasovskii Functionals For Linear Time Delay Systems," *American Control Conference*, vol. 4, pp. 2845–2850, 2005.

[12] P. D. Groves, *Principles of GNSS, Inertial, and Multisensor Integrated Navigation Systems*. Artech House, 2013.

[13] D. B. Kingston and R. W. Beard, "Real-Time Attitude and Position Estimation for Small UAVs Using Low-Cost Sensors," *American Institute of Aeronautics and Astronautics, "Unmanned Unlimited"*, vol. -, pp. 1–9, 2004.

[14] A. Ailon and S. Arogeti, "Study on the effects of time-delay on quadrotor-type helicopter dynamics," *Mediterranean Conference on Control and Automation (MED)*, vol. -, pp. 305–310, 2014.

[15] A. Khosravian, J. Trumpf, R. Mahony, and T. Hamel, "Velocity Aided Attitude Estimation on SO(3) with Sensor Delay," *IEEE Conference on Decision and Control*, vol. 14, pp. 114–120, 2014.

[16] ——, "Recursive Attitude Estimation in the Presence of Multi-rate and Multi-delay Vector Measurements," *American Control Conference*, vol. -, pp. –, 2015.

[17] A. Khosravian, J. Trumpf, R. Mahony, and C. Lageman, "Observers for Invariant Systems on Lie Groups with Biased Input Measurements and Homogeneous Outputs," *Automatica*, vol. -, pp. –, 2015.

[18] H. F. Grip, T. I. Fossen, T. A. Johansen, and A. Saberi, "Attitude Estimation Using Biased Gyro and Vector Measurements With Time-Varying Reference Vectors," *IEEE Transactions on Automatic Control*, vol. 57, pp. 1332–1338, 2012.

[19] ——, "Nonlinear Observer for GNSS-Aided Inertial Navigation with Quaternion-Based Attitude Estimation," *American Control Conference*, vol. -, pp. 272–279, 2013.

[20] T. I. Fossen, *Handbook of Marine Craft Hydrodynamics and Motion Control*. John Wiley & Sons, Ltd, 2011.